The influence of fiber dimensions on mechanical pulp long fiber tensile index and density

Sofia Reyier Österling, Olof Ferritsius, and Rita Ferritsius

KEYWORDS: Mechanical pulp, Bonding ability, Fiber characterization, Sheet properties, Optical analyzer, FiberLab, SEM image analysis, MorFi Lab, Fibrillation, Fiber width, Fiber wall thickness, Collapse resistance

SUMMARY: This study discusses how fiber dimensions affect the tensile index and density of long fiber laboratory sheets. Five commercial mechanical pulps (three TMP grades, one SGW and one CTMP) were fractionated into five streams in a hydrocyclone pilot plant. Fiber dimensions and fibrillation were analyzed of the P16/R30 and P30/R50 fractions and compared to the sheet properties. For comparison, samples were also analyzed by SEM cross-sectional image analysis and in a MorFi Lab optical analyzer.

Fibrillation index showed a high positive influence on long fiber tensile index and density, whereas fiber wall thickness, fiber width, and collapse resistance index a negative. Fiber width showed the vaguest correlation to long fiber tensile index and density of the analyzed fiber properties, but this increased when combined with fiber wall thickness into collapse resistance index, CRI. The correlations between fiber properties and sheet properties were on different levels for the different mechanical pulping processes, but a combination of collapse resistance index and fibrillation index into the novel factor *BIN*, Bonding ability INfluence, gave one linear relation of high correlation to long fiber tensile index for all pulps, except the SGW P30/R50 fraction, which showed the same linear correlation on a slightly lower level. BIN should be a useful tool in characterizing mechanical pulp fibers.

ADDRESSES OF THE AUTHORS: Sofia Reyier Österling (sofia.reyier-osterling@storaenso.com), Stora Enso Printing and Reading Mechanical Fiber R&D, Kvarnsveden Mill, SE-78183 Borlänge, Sweden; FSCN Mid Sweden University, SE-85170 Sundsvall, Sweden, **Olof Ferritsius**, FSCN Mid Sweden University (former Pöyry Sweden AB), **Rita Ferritsius**, Stora Enso Kvarnsveden mill, SE-78183 Borlänge, Sweden; FSCN Mid Sweden University (former Pöyry Sweden AB).

Corresponding author: Sofia Reyier Österling

In a mechanical pulp, the characteristics of the long fibers have a strong influence on the characteristics of sheets from whole pulps (see e.g. Mohlin 1989, Rundlöf 2002). Demands are increasing for printing paper surface and strength and at the same time, higher demands are also put on the mechanical pulping process energy efficiency. To be able to optimize both the printing paper quality and the process efficiency with respect to electrical energy input, detailed knowledge of fiber properties is required. The demands on fiber dimensions are different for different mechanical pulp end products, and also differ between mills depending on raw material, process types, and furnish composition (Höglund and Wilhemsson 1993, Reyier et al. 2011). To improve the possibilities to optimize the mechanical pulping process and fiber treatment, appropriate methods to evaluate the pulp and fiber properties are needed.

In 1989, Mohlin highlighted the key parameter in producing mechanical pulps for printing paper as the fiber bonding ability, defined as "Bonding index", the tensile index of long fiber fraction P16/R30 using the Bauer McNett fractionator. Fiber bonding ability in mechanical pulps as discussed in this study refers to the fibers' ability to come close enough to other fibers and fiber material to interact and form dense sheets of high strength. This report discusses fiber bonding ability as evaluated through long fiber sheet properties. The nature of the interactions which join together the mechanical pulp fibers is outside the scope of this work.

In 1963, Forgacs demonstrated how to use linear regressions to calculate burst, tear, bulk and wet web strength using the S- and L-factors. The L-factor, length, referred to the fraction retained on a 48-mesh screen, and the S-factor, shape, was defined as the specific surface of the P48/R100 Bauer McNett fraction. The specific surface was derived from permeability measurements of fiber beds while fiber length was calculated from microscopy analysis. In 1987, Strand showed that about 95% of the variations in pulp properties could be explained by two factors, Factor 1 and Factor 2. Factor 1 correlated to Forgacs' S-factor (shape, i.e. corresponding to bonding ability) and Factor 2 to Forgacs' L-factor (length). Ferritsius and Ferritsius (1996, 1997, 2001) applied the work of Strand at some Stora Enso mills, predicting the independent factors F1 and F2 to control the process in order to produce uniform pulp quality.

Long fiber laboratory sheets for fiber characterization have been useful in understanding pulping processes mechanisms and furnish optimization (Mohlin 1980, 1997, Reyier et al. 2011). Making long fiber sheets and testing them is however a time consuming process and therefore not practical in daily evaluations of mechanical pulp processes. Cross-sectional SEM image analysis has also proven valuable for fiber evaluations reflecting on the pulping process (Reme, Helle 2001, Kure et al. 1999) but it requires significant analyzing time and highly skilled technicians. Analyzing fiber properties in optical analyzers enables faster fiber characterization, independent of both laboratory and technician performance. Optical analyzers also enable the evaluation of high-resolution distributions of fiber properties (Reyier 2008, 2011) and simplified division into different fiber types (Lhotta et al. 2007).

The purpose of this study was to evaluate how geometrical fiber dimensions influence the physical properties of long fiber laboratory sheets, mainly the long fiber tensile index and density, using different methods of fiber characterization.

Materials and Methods

Materials

Five screened and reject refined commercial final pulps of Norwegian Spruce (*Picea Abies*) were fractionated in hydrocyclones. The five pulps, described in *Table 1*, were selected for the large disparities between the pulps in both average fiber length and fiber bonding ability, to widen the fiber characteristics of the pulps used in this study. Differences between the five pulps were large both in specific energy consumption, process design and final product requirements.

The five pulps' fiber fraction composition as evaluated in the Bauer McNett device is seen in *Fig 1*. The height of the bars indicate the total amount of fibers and fibrous material retained on a 100 mesh wire, R100, for each pulp. As expected, the CTMP showed the highest amount of R100 fraction, about 78% of the total pulp and the SGW the lowest, 47%. The three TMPs were placed between the SGW and CTMP.

Methods

The five mechanical pulps were processed through a four-stage hydrocyclone pilot plant at Noss AB in Norrköping, Sweden. Hydrocyclones have been found to separate fibers according to fiber wall thickness and specific surface (Karnis 1981, Kure et al. 1999, Shagaev, Bergström 2005). Each pulp was fractionated into five streams; the first accept stream was denoted "stream 1" and the last reject "stream 5", *Fig 2*. TMP1 was used as a reference pulp and hydrocyclone settings were adjusted so that approximately 20% of the R100 fibers of TMP1 went with each hydrocyclone stream. TMP2, TMP3, SGW, and CTMP were then processed through the hydrocyclone setup utilizing the same settings.

Table 2 shows the amounts (mass-% of feed pulp) of the Bauer McNett P16/R30 and P30/R50 fractions in each hydrocyclone stream. The fractionation showed that for TMP1 approximately 20% of these fiber fractions were found in each stream. For TMP2; stream 1 contained about 30 mass-% of the fibers and then successively lower amounts until the last reject, stream 5. The fractions of TMP3 and SGW (both SC grade) were divided quite similarly in the fractionation with most material found in the first two hydrocyclone streams, whereas for the CTMP, most of the feed pulps' P16/R30 and P30/R50 fractions were found in streams 4-5.

Table 1. Pulps used in this study.

Denotation	Pulp type, description
TMP1	News grade single stage conical disc refined TMP, about 1900 kWh/ADMT.
TMP2	News grade single stage double disc refined TMP, about 1900 kWh/ADMT.
TMP3	Magazine grade two stage double disc refined TMP, about 3000 kWh/ADMT.
SGW	Magazine grade atmospheric grinded SGW, about 1900 kWh/ADMT.
CTMP	Paper-board mid layer sulphite pre-treated conical disc refined CTMP, about 1000 kWh/ADMT.

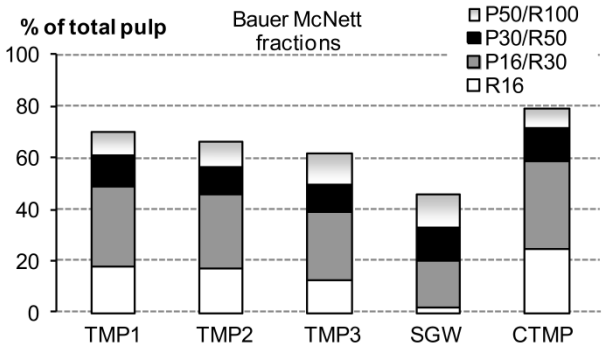

Fig 1. Fiber fraction composition as evaluated in a Bauer McNett classifier. Bar height represent amount of R100 fibers for each pulp. As expected, the CTMP had the highest amount of R100 material whereas the SGW had the lowest. The three TMPs were placed between the SGW and CTMP.

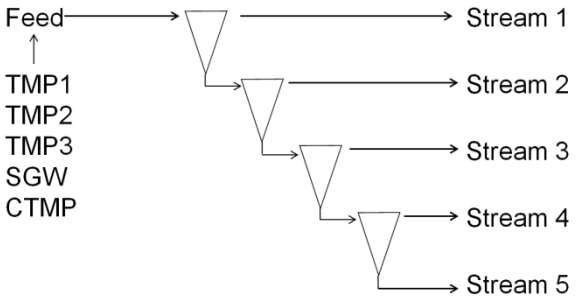

Fig 2. The four-stage hydrocyclone pilot fractionation was designed to give five streams from each feed pulp. TMP1 was used as a reference and hydrocyclone settings were adjusted so that approximately 20% of the TMP1 R100 fibers went with each hydrocyclone stream. The same hydrocyclone settings were then used for all pulps in the study.

Table 2. The P16/R30 and P30/R50 fractions were divided into the five hydrocyclone streams depending on each pulp's fiber bonding ability. For the two SC grade pulps, TMP3 and SGW, the highest amounts of the P16/R30 and P30/R50 fractions were found in the first two streams, suggesting pulps of high fiber bonding ability. For the CTMP, most fibers and fibrous material was found in the last two streams, suggesting lower fiber bonding ability of the CTMP.

Weight percent of feed pulp [%]						
Stream #		1	2	3	4	5
TMP1	P16/R30	22.4	20.6	23.3	16.5	17.1
	P30/R50	24.5	19.7	21.8	14.9	19.1
TMP2	P16/R30	29.1	24.3	16.9	10.7	19.1
	P30/R50	31.8	24.6	15.5	11.4	16.7
TMP3	P16/R30	47.2	29.1	13.3	5.8	4.6
	P30/R50	50.5	28.6	12.1	4.9	3.9
SGW	P16/R30	49.5	31.5	10.4	4.0	4.7
	P30/R50	49.4	31.4	9.7	3.5	6.0
CTMP	P16/R30	4.2	9.0	5.2	29.6	41.9
	P30/R50	6.7	8.5	6.3	36.0	42.5

The way the material was divided in the five hydrocyclone streams can be seen as a measure of each pulp's fiber bonding ability (Reyier et al 2008) and the division of the pulps suggest high fiber bonding ability of the two SC grade pulps and low for the CTMP.

After hydrocyclone fractionation, the pulp fractions from each hydrocyclone stream and the feed were dewatered on a 200 mesh wire and by a centrifuge to above 30% dry content and frozen in plastic bags in -28˚C. Before use, the pulps were hot disintegrated (ISO 5263-3) and then fractionated in a Bauer McNett device (SCAN-CM 6:05) equipped with 16, 30, 50, and 100 mesh wires. The Bauer McNett fractionation was performed in order to characterize the fiber bonding ability with limited influence of fiber length. It has been shown that the Bauer McNett fractionator separate fibers mainly with respect to fiber length but also to some extent by flexibility (Petit-Conil et al. 1994).

Since the first Bauer McNett fraction, R16, without any upper limit, may have contained untreated fiber material and shives, and the material passing the 50 mesh screen may have lost some of its fiber character (Mohlin 1980), evaluations were focused on fibers from the P16/R30 and P30/R50 fractions. Despite differences in fiber length between the pulps and wide fiber length distributions for the P16/R30 and P30/R50 fractions, the Bauer McNett, the Bauer McNett fractionation resulted in two separate fiber length levels of the P16/R30 and P30/R50 fractions. *Table 3* below shows the range of the average (arithmetic average) fiber length from stream 1 (first accept) to stream 5 (last reject) for the five evaluated pulps. Fiber lengths shown in *Table 3* are based on FiberLab data selected in accordance with the description in the next section, and includes only material where the cross-sectional fiber wall area, fibrillation index and curl could be determined in the image analysis.

From the Bauer McNett fractions of each hydrocyclone stream and feed, long fiber laboratory sheets were formed (ISO 5269-1 earlier SCAN CM26:99). The long fiber sheets were evaluated for tensile index in an L&W Alwetron TH1 (SCAN-P 67) and density in a STFI thickness measurement device (SCAN-P 88:01). To avoid deviations which may be induced by different routines in the handling of the samples, all laboratory sheets were produced and tested by the same technician.

Table 3. Range of average fiber length* (excluding fines) of the five hydrocyclone streams, P16/R30 and P30/R50 fractions. Despite wide distributions of fiber length in the Bauer McNett fractions, two separate levels were formed for the P16/R30 and the P30/R50 fractions.

Range of average fiber length [mm]* Stream1→5	**TMP1**	**TMP2**	**TMP3**	**SGW**	**CTMP**
P16/R30	1.84-1.96	1.86-1.89	1.79-1.82	1.79-1.82	1.95-2.09
P30/R50	1.11-1.13	1.13-1.13	0.98-1.07	1.09-1.09	1.13-1.18

*based on FiberLab data where the cross-sectional fiber wall area, curl and fibrillation index could be determined by image analysis.

The P16/R30 and P30/R50 fractions of all samples including feed pulps were processed through an optical measurement device, Metso Automation FiberLab™. In the FiberLab device, values of fibrillation index, fiber wall thickness index, fiber width index, and two measures of fiber length are obtained through an image analysis system using two perpendicular cameras (Kauppinen 1998, FiberLab Operating manual 2002). The two fiber length measures are "true" fiber length; fiber length along the fiber center, and projected fiber length, the shortest distance between the two fiber ends. In the measurement, diluted fiber samples are sucked from a measurement cup into a measurement capillary, in which the fiber passes through a polarized laser beam. The light polarization changes when a fiber passes the beam and a detector behind an absorbent filter registers the altered polarization light. An image proportional to fiber length is formed and converted to digital form and an amplified detector signal then gives a value of fiber length. The length measurement settings used in the FiberLab analysis in this study ranges from 0.2-7.6 mm with a resolution of 50µm. When a fiber is in position to be analyzed, a xenon lamp flashes and a CCD (charged coupled device) camera takes a photo of the middle part of the fiber. Average fiber width and fiber wall thickness is calculated by grey level differences from 40 measurements of the middle 0.7 mm of each fiber (Kauppinen 1998). The cross-sectional dimensions measurement resolution is 1µm. Fibrillation index of each fiber is calculated as the ratio between area of fibrils and area of fiber body plus fibrils with a resolution of <0.1µm using grey scale sub-pixel calculations to define the area of fibrils. The FiberLab measurement chamber is outlined in *Fig 3* redrawn from Kauppinen (1998).

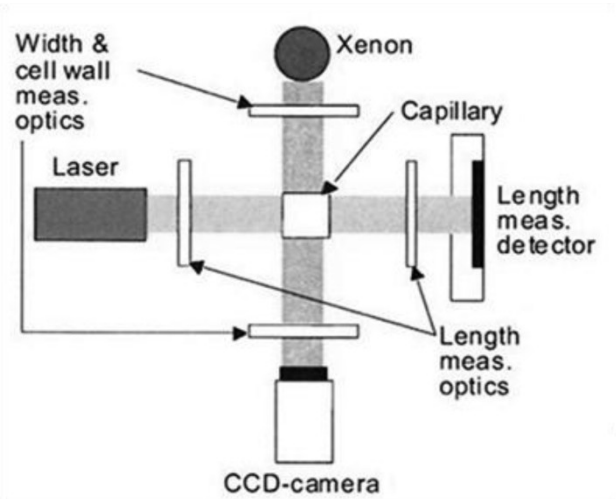

Fig 3. FiberLab measurement chamber outlined by Kauppinen (1998). A diluted fiber solution is sucked into a measurement capillary and passes a laser beam that registers the fiber passage. Two measurements of fiber length are analyzed by a projected image proportional to the fiber length. The fiber wall thickness and width is obtained from image analysis of grey scale differences of 40 images of the middle 0.7 mm of the fiber, produced by a CCD camera combined with a xenon flash. The fibrillation index is calculated as the ratio between area of fibrils and area of fiber body plus fibrils, using sub-pixel calculations of grey-scale images.

The result of the CCD camera image analysis is synchronized with results of fiber length for each analyzed fiber and stored in a result file. Each measurement produces a default printout report of averages and rough histograms of the pulp properties, based on fibers as well as fines and parts of fibrils. In this study the raw data files were also imported into a data base from which results were refined as described below, in order to evaluate fiber properties without the influence of fines or broken fiber parts. Values of fiber wall thickness and fiber width from the FiberLab device are relative values and are referred to in this study as indexes.

Before FiberLab analysis, fiber samples were diluted to 0.16 g/l in a 5000 ml container from which 50 ml was used for each measurement. This study was based on results from 9-12 FiberLab measurements per sample to ensure a high number of evaluated fibers. FiberLab results of samples from the P30/R50 fraction of stream 3 from TMP2 and CTMP were not included in results due to sample handling mistakes.

By default, fibrillation index is not evaluated for all particles in the FiberLab device. For some particles, fibrillation index was also measured but the results were rejected by the software settings, for example because of too short a fiber length. For statistical validation in producing distributions based on fibrillation index, only fibers with a measured fibrillation index were included in the results. This study was focused on fibers, not fines or non-fibrous material, and data base selections were performed in such ways as to ensure that fine material included in FiberLab measurements was not included in the results. Therefore, only measured material with a saved image analysis result of cross-sectional fiber wall area were included in the results, excluding broken parts of fibers as well as fine material. By this selection process, FiberLab results were also comparable to results of cross-sectional image analysis methods, where only fibers with a measurable (intact) perimeter and fiber wall thickness were included in the evaluation. Further, fibers of fiber curl zero, fiber curl defined as the calculated ratio between true and projected fiber lengths minus 1 (expressed in percent), were not included in the results as a fiber curl of zero was considered an indication of measurements disturbances. The fiber curl is a longitudinal measure of the fiber and does not include or influence the characterization of any cross-sectional fiber dimensions.

The FiberLab data was used to calculate more fiber dimensions based on cross-sectional fiber properties. Collapse resistance index, CRI, was calculated for each fiber according to the equation suggested by Gradin together with Vesterlind and Höglund (Vesterlind and Höglund 2005), *Eq 1*.

$$CRI_i = \frac{1}{N}\sum_{i=1}^{N}\frac{fiber\ wall\ thickness_i^{\,2}}{fiber\ width_i - fiber\ wall\ thickness_i} \qquad [1]$$

Below is an outline of how the fiber wall thickness index and the fiber width index were evaluated and apparent differences between high and low collapse resistance index CRI, *Fig 4*.

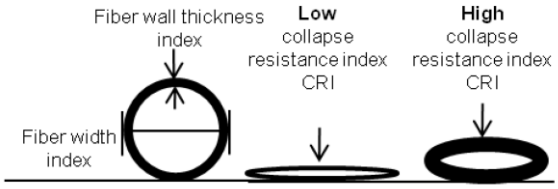

Fig 4. Outline of analysis of fiber wall thickness and fiber width and illustration of the differences between high and low collapse resistance index CRI.

Table 4. Example of 95% confidence intervals of ten FiberLab measurements per sample for a high energy SC grade pulp with similar properties as TMP3.

95% confidence intervals from ten FiberLab measurements

	Fiber length	Fibrillation index	Fiber wall thickness index	Fiber width index
95% conf. interval	0.007	0.03	0.08	0.08

All fiber properties analyzed using the FiberLab were calculated based on single fiber measurements of 30 000 - 60 000 fibers per sample (corresponding to 9-12 FiberLab measurements per sample). *Table 4* shows an example of confidence intervals for FiberLab averages of fibrillation index, fiber wall thickness index and fiber width index, based on 10 measurements per average of a high energy SC grade pulp with similar properties as TMP3 used in this study.

For method comparisons regarding fiber width, fiber samples were also processed through a MorFi Lab optical analyzer (Eymin Petot Tourtollet et al. 2003) at CTP, Grenoble, France. The MorFi Lab results are averages obtained using default settings without the data selection that was often made for the FiberLab results, and the MorFi Lab results were therefore compared to default setting averages from the FiberLab. MorFi Lab results included in this study were based on about 5 000 fibers per sample.

For method comparisons regarding analysis of fiber wall thickness and fiber width, cross-sectional scanning electron microscopy, SEM, images were prepared and analyzed at Stora Enso Research Centre, Falun, Sweden, in accordance with internal methods based on the method described by Reme and Helle (Reme 2000, Reme and Helle 2001). The P16/R30 fraction fibers were aligned into fiber bundles, then rapidly dry frozen by liquid nitrogen. To ensure less than 1% water content in the samples, the fiber bundles were kept at 60-70˚C in an oven for one hour, and then embedded in epoxy to maintain the wet fiber appearance. Thin cross-sectional slices were cut from the embedded fiber bundles after which the slices were polished and processed to digital images in a SEM. The grey scale images were then made binary and evaluated by a semi-automatic, internally developed, image analysis method in which cross-sectional fiber dimensions of each fiber with an intact perimeter and fiber wall were analyzed. Before the image analysis, individual fibers which were in contact with each other were separated by a one-pixel line and fine material, noise and longitudinally aligned fibers was

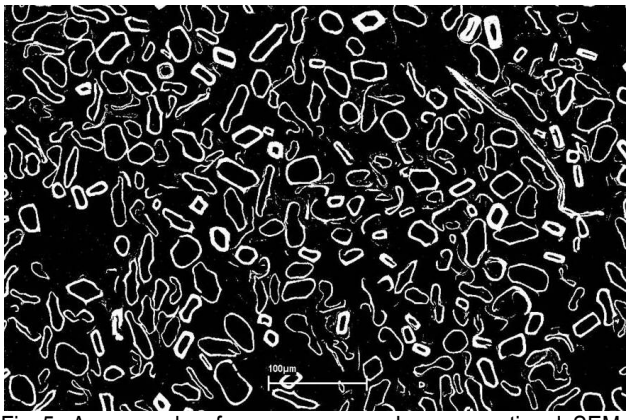

Fig 5. An example of a non-processed cross sectional SEM micrograph of the TMP1 P16/R30 fraction. The image shows a wide distribution in fiber dimensions both with respect to fiber wall thickness and fiber width. Grey-scale cross-sectional SEM images were used to quantify the fiber wall thickness and fiber width by an internally developed method based on the method described by Reme and Helle (Reme 2000, Reme and Helle 2001).

removed from the images. Shives were separately identified and removed from the analysis image, and pits seen as small ruptures in the fiber walls were filled to be able to analyze the fiber as to have an intact wall. Cross-sections of broken fibers were removed from the analysis image and fully collapsed fibers were given an "artificial lumen" by a one pixel line. Results from the cross-sectional SEM image analysis in this study were based on 600-1200 fibers per sample. One example of a cross-sectional SEM micrograph of TMP1 before image processing is found in *Fig 5*. It can also be observed the wide distribution in fiber wall thickness and fiber width within the sample.

The wide distribution in mechanical pulp fiber dimensions makes standard deviation a less suitable measure of the wideness of these distributions, which in addition have seldom been found to be normally distributed. Instead, to estimate the wideness of the distributions of fiber properties, the difference between percentile 0.95 and percentile 0.05, defined as the F0.90 (Ferritsius et al. 2009) was used, *Eq 2*.

$$F0.90 = Percentile\,0.95 - Percentile\,0.05 \qquad [2]$$

To visually observe differences between some of the hydrocyclone streams, SEM images of P16/R30 Formette (Formette dynamic sheet former) sheets were produced. Sheet samples 1*1 cm in size, covered with a thin layer of a gold and palladium mixture were used for the micrographs, which were made with the sample angled at 20˚ in the SEM to enhance structural characteristics.

Results

Handsheet properties

Evaluations of the hydrocyclone fractionation showed that the hydrocyclones efficiently separated the fibers with respect to fiber dimensions, both reflected in averages from the FiberLab analyses and evaluations of sheet properties. The distributions of fiber dimensions both within the feed pulps and within the hydrocyclone streams were however wide, for all pulps. *Figs 6a* and *b*

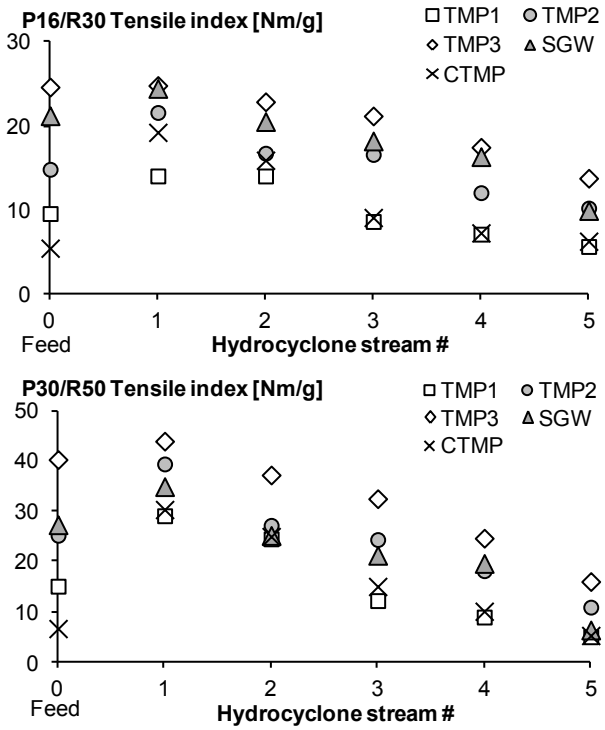

Fig 6a and 6b. Properties of handsheets made from the hydrocyclone fractionated pulps showed that the hydrocyclone were efficient in separating the fibers. The tensile index of both the P16/R30 (Fig 6a) and P30/R50 (Fig 6b) fractions was highest for stream 1, the first accept, and lowest for fibers from stream 5, the last reject.

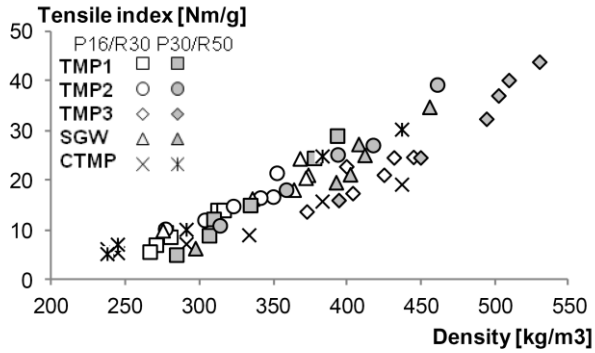

Fig 7. There was a linear correlation between density and tensile index of the P16/R30 and P30/R50 fractions of five hydrocyclone fractionated pulps.

shows the tensile index of handsheets made of the P16/R30 and P30/R50 fractions respectively. For all pulps, the tensile index was highest in stream 1 (first accept) for both the P16/R30 and P30/R50 fractions and then successively lower for each hydrocyclone stream to stream 5 (last reject, c.f. *Fig 2*). The amount of fibers in each hydrocyclone stream differed between the pulps, c.f. *Table 2*.

The tensile index showed a linear relation to sheet density, *Fig 7,* which was also expected based on the results of Höglund and Wilhemsson (1993) in evaluations of whole pulps and Rundlöf (2002) for sheets with different fines contents.

The CTMP P16/R30 fraction showed slightly lower increase of tensile index with increasing density than the

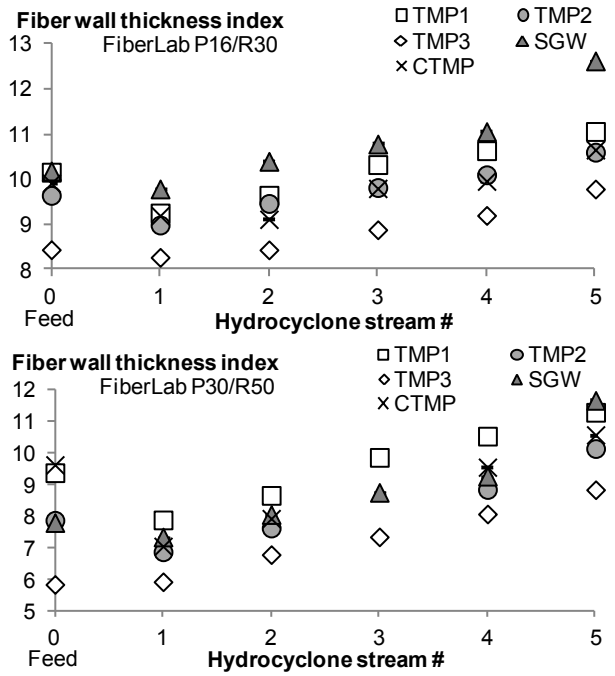

Fig 8a and 8b. Fibers in the last hydrocyclone reject, stream 5, had the highest average fiber wall thickness index and fibers in the first accept stream, stream 1, had the lowest fiber wall thickness index for the P16/R30 and P30/R50 fractions of all pulps.

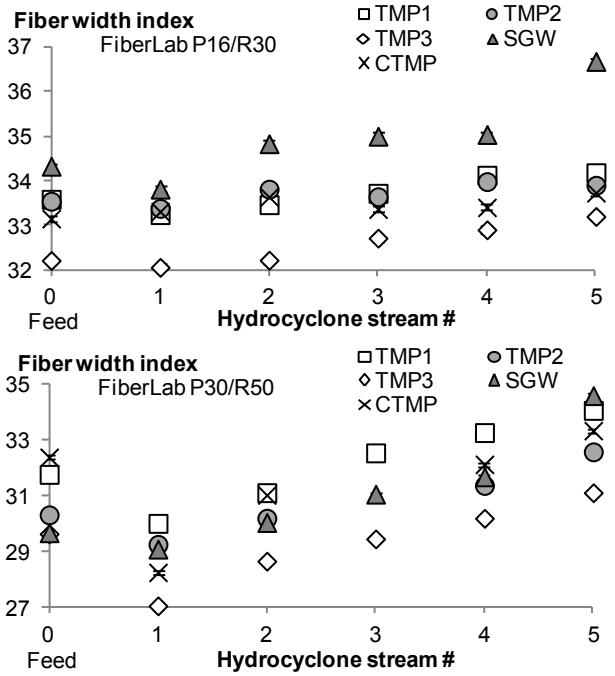

Fig 9a and 9b. Average fiber width index was highest for the fibers in the last reject stream (stream 5) and lowest for the fibers in the first accept stream (stream 1) for the P16/R30 and P30/R50 fractions of all pulps.

other evaluated pulps. The SC grade TMP (TMP3) showed both the highest long fiber tensile index and density. TMP3 and the SGW P30/R50 fraction showed a slightly higher density at a given tensile index than the other pulps. This may be a result of higher fiber flexibility or collapsibility, but it is also possible that these observations were influenced by the fractionation process, and these observations are recommended to be further evaluated. For both the tensile index and density, differences between stream 1 and stream 5 were larger for the P30/R50 fractions than for the P16/R30 fractions. This is further discussed in the evaluation of fiber dimensions below.

Fiber properties

Evaluations of arithmetic averages of fiber dimensions from the FiberLab analyzer showed that fiber wall thickness index (*Fig 8a, b*), fiber width index (*Fig 9a, b*), and collapse resistance index (*Fig 10a,b*) increased from stream 1 to stream 5 for both the P16/R30 and P30/R50 fractions. In contrast, the fibrillation index decreased from stream 1 to stream 5 (*Fig 11a, b*). Small numerical differences in fibrillation index represent significant and visually large differences in external fibrillation.

Of the evaluated pulps, the SGW fibers showed the highest fibrillation index for both the P16/R30 and the P30/R50 fractions. The SGW fibers also showed high collapse resistance index and for the P16/R30 fraction, the highest collapse resistance index of the five evaluated pulps. Among the TMPs, the TMP of highest fibrillation index, the SC grade pulp TMP3, also showed the lowest fiber wall thickness index, fiber width index and collapse resistance index. Results from the hydrocyclone

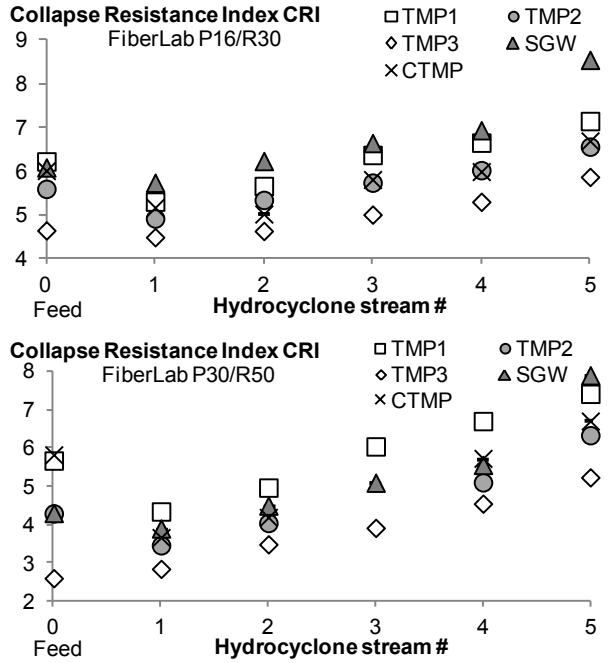

Fig 10a and 10b. Average collapse resistance index was highest for the fibers in the last reject stream (stream 5) and lowest for the fibers in the first accept stream (stream 1) for the P16/R30 and P30/R50 fractions of all pulps.

fractionation support earlier findings that hydrocyclones mainly fractionate material based on gravity and specific surface (Karnis 1981, Kure et al. 1999, Shagaev and Bergström 2005), which means that fibers of highest fibrillation index and lowest fiber wall thickness should be expected to end up in the first hydrocyclone accept. It is possible that also the fiber split may influence the long fiber tensile index and density and there may be

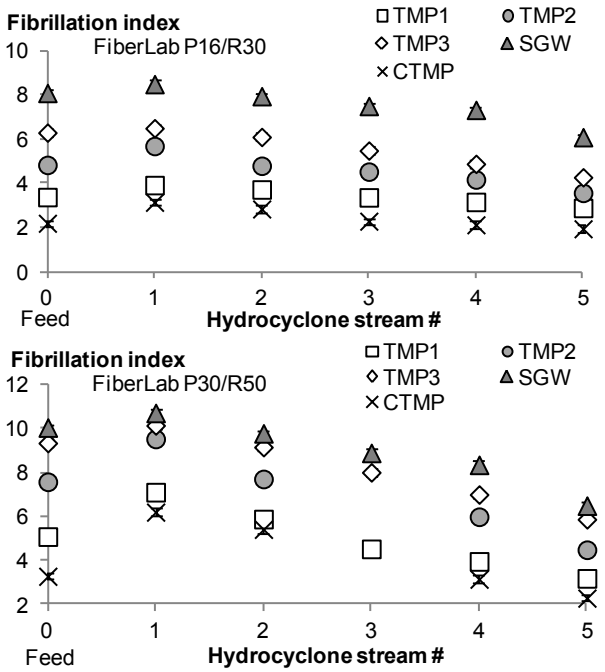

Fig 11a and 11b. Average fibrillation index was highest for the fibers in the first accept stream (stream 1) and lowest for the fibers in the last reject stream (stream 5) for the P16/R30 and P30/R50 fractions of all pulps. Small numerical differences in fibrillation index represent significant and visually large differences in external fibrillation.

differences in fiber split between fibers from TMP and SGW processes as well as from different process designs. As the fiber split is not distinguishable in the optical fiber analysis method used in this study, this is recommended as something to look further into when fast, accurate methods of identifying fiber split of a large number of fibers become available.

From the results seen in *Figs 8-11*, it seems that differences in arithmetic average values between stream 1 and stream 5 were larger for the fibers of the P30/R50 fraction than for the P16/R30 fraction, for all fiber dimensions evaluated here. This may indicate that hydrocyclones are more efficient in fractionating shorter fibers, and/or that there are in fact broader distributions of fiber dimensions in the P30/R50 fraction than in the P16/R30 fraction. *Table 5a* and *5b* shows the distribution wideness (F0.90) of the distributions of fiber wall thickness index (*Table 5a*) and fibrillation index (*Table 5b*), for the P16/R30 and P30/R50 fractions of the five feed pulps. It can be seen that fiber wall thickness index as evaluated in the FiberLab device had a broader distribution for the P16/R30 fraction than for the P30/R50 fraction, whereas for fibrillation index the distribution was wider for the P30/R50 fraction than for the P16/R30 fraction. These results are reported as observations to be followed by a more thorough evaluation.

To give a qualitative view of the differences in appearance between fibers from stream 1 and stream 5, SEM micrographs of handsheets of P16/R30 stream 1 and 5 of TMP2 are shown in *Fig 12a* and *12b*. The first hydrocyclone accept fibers (stream 1, *Fig 12a*) appear to be more collapsed and give a denser network than the last hydrocyclone reject fibers, stream 5, *Fig 12b*.

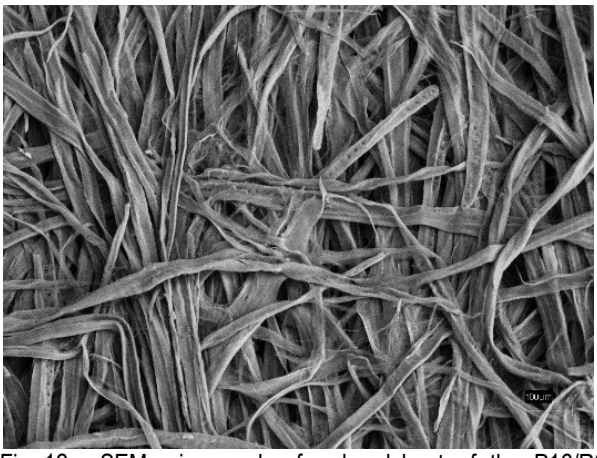

Fig 12a. SEM micrograph of a handsheet of the P16/R30 fraction of the first hydrocyclone accept stream (1) of TMP2. The image shows a dense sheet of seemingly flexible fibers of high fibril content of 300x magnification (scale bar in the lower right corner indicating 100µm).

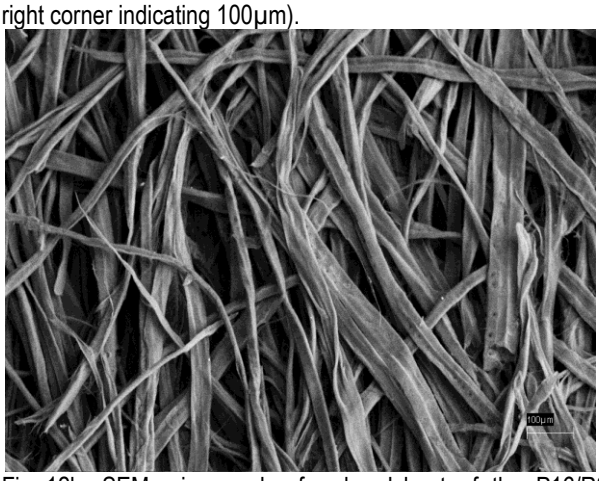

Fig 12b. SEM micrograph of a handsheet of the P16/R30 fraction of the last reject hydrocyclone stream (5) of TMP2, Compared to the sheet in *Fig 12a*, a more open sheet with lower degree of fiber-fiber interaction of 300x magnification (scale bar the lower right corner indicating 100µm).

Tables 5a and 5b. Distribution wideness (F0.90) for fiber wall thickness index and fibrillation index for the P16/R30 and P30/R50 fractions of the five feed pulps.

Distribution wideness F0.90, fiber wall thickness index

	TMP1	TMP2	TMP3	SGW	CTMP
P16/R30	17.6	16.8	16.8	19.2	16.0
P30/R50	16.8	16.0	14.7	17.6	16.0

Distribution wideness F0.90, fibrillation index

	TMP1	TMP2	TMP3	SGW	CTMP
P16/R30	11.1	16.5	21.6	19.5	8.2
P30/R50	18.2	24.4	28.3	25.3	13.3

Cross-sectional SEM image analysis

Cross-sectional SEM image analysis of fiber wall thickness and fiber width was performed on the P16/R30 fractions of feed, stream 1, and stream 5 of all the five pulps. For fiber wall thickness, the ranking of the feed, first accept and last reject was the same using the SEM image analysis method as with FiberLab for each pulp, (c.f. *Fig 8a*) which was expected considering that hydrocyclones are known to separate fibers with respect

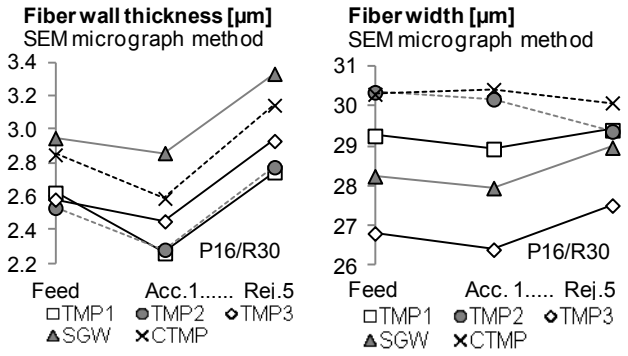

Fig 13a and 13b. Results of analysis of fiber wall thickness and fiber width from SEM micrographs showed the expected lowest average fiber wall thickness in the first accept (1) and the highest in the last reject (5), the same ranking as from the FiberLab analysis. The ranking of the fiber width was however in contradiction to the FiberLab results for two of the pulps. Differences in average fiber width between feed, accept 1 and reject 5 were small.

to fiber wall thickness. The ranking between the pulps was however different with the SEM method compared to the FiberLab method. SGW was still the pulp of the highest wall thickness, but TMP1 and TMP2 were ranked as having lower fiber wall thickness than TMP3 in the SEM analysis, *Fig 13a*. For fiber width, the differences between stream 1, 5 and feed were small both with the FiberLab and the SEM analysis. For three pulps, the ranking between stream 1, 5 and feed were the same as from the FiberLab analysis, whereas for two pulps, CTMP and TMP2, the lowest fiber width was seen in stream 5, in contradiction to the FiberLab results, *Fig 13b*. None of the changes in ranking were judged to be related to the processes from which the samples were collected.

Unpublished results have shown that weight weighted averages of FiberLab fiber width (as opposed to arithmetic averages as presented in this evaluation) for some of the fractionated pulps resulted in the same change in ranking between stream 1 and stream 5 as seen for CTMP and TMP2 in the SEM analysis (c.f. *Fig 13*). If this has any connection to the altered ranking seen here is not clarified. Differences in fiber width between the hydrocyclone streams were small using the SEM image analysis method, whereas differences between the streams in laboratory sheet properties, fiber wall thickness index from FiberLab and fibrillation index from FiberLab were obvious. Differences in ranking of fiber width between the FiberLab and the cross-sectional SEM image analysis methods are not considered central to the results of this study, but are included to show how the ranking of fiber dimensions in pulps may sometimes differ depending on the utilized method.

Fig 14a shows the correlation between results from FiberLab and SEM analyses of fiber wall thickness. All pulps gave linear relations between the two methods of analysis. The three TMPs showed approximately the same slope but on different levels. The two news-grade fiber types, TMP1 and TMP2, gave approximately the same linear relation whereas the high energy TMP3 gave

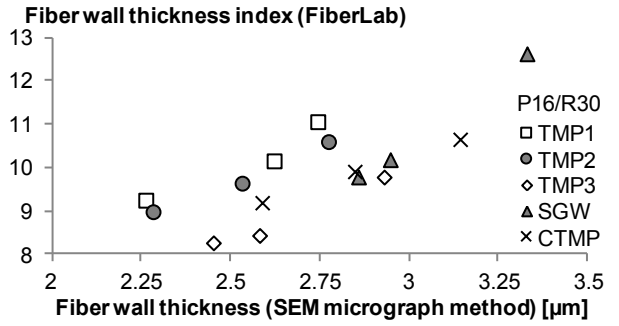

Fig 14a. Comparisons of fiber wall thickness from FiberLab and cross-sectional SEM micrograph analysis methods for the P16/R30 fractions of feed, stream 1 and stream 5 of all pulps.

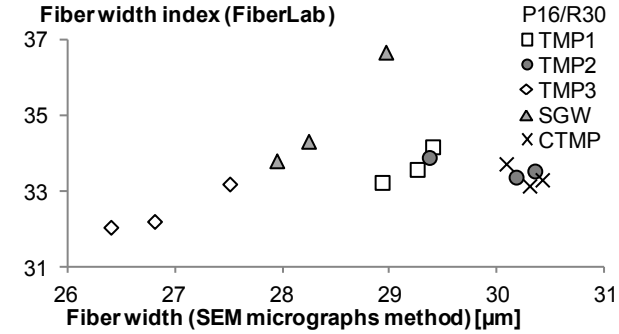

Fig 14b. Comparisons of fiber width from FiberLab and cross-sectional SEM micrograph analysis methods for the P16/R30 fractions of feed, stream 1 and stream 5 of all pulps. TMP3 and SGW, the SC grade pulps, appeared to fall on the same line whereas TMP1 was on a lower level. The SEM method showed the same ranking as FiberLab for TMP3, SGW and TMP1 whereas SGW and CTMP showed small differences in fiber width for both methods and no correlation to the FiberLab results.

a similar slope of correlation but on a lower level, the same as that of the SGW. Despite the absolute value differences, rankings of feed, stream 1 and stream 5 remained.

Fig 14b shows a similar plot for fiber width. In this case, TMP3 and SGW, the SC grade pulps, appeared to fall on the same line and data for TMP1 suggested a linear relation at a lower level, corresponding to the ranking seen in the FiberLab evaluations. Both the cross-sectional SEM image analysis and the FiberLab methods showed small differences for TMP1 and CTMP. TMP2 and CTMP, that showed diverging trends for feed, stream 1 and stream 5 in the cross-sectional SEM analysis method compared to the FiberLab results, showed no correlation between FiberLab and cross-sectional SEM image analysis results for fiber width.

The cross-sectional SEM image analysis method used in this study showed some correlation to FiberLab results of fiber wall thickness and fiber width, however with some exceptions and on different levels for different pulps. For fiber wall thickness, the internal ranking of accept, reject and feed was the same for the FiberLab and cross-sectional SEM image analysis, whereas the fiber width data showed small differences between the streams and also changed the ranking of the streams for two pulp.

The same measurement approaches were used for the cross-sectional SEM image analysis method and the FiberLab method and only fibers with intact fiber walls were included in the results of both methods. Also the first part of the sample preparation was performed in identical ways for hot disintegration and collection of long fiber fractions in the Bauer McNett classifier. Prior to both analysis methods, fibers were stored in a low consistency dilution at least 20 minutes, which should have contributed to low amounts of fully collapsed (no distinguishable lumen) fibers.

In the FiberLab method, if a lumen area is not recognized by the cross-sectional camera, the data is rejected by the image analysis default settings. In the cross-sectional SEM image analysis method, if a fully collapsed fiber with no distinguishable lumen was encountered, a "fake lumen" was introduced in the image analysis as a line, one pixel in width, in the middle of the cross-section before the fiber width was measured. This may have contributed to the differences between the methods. The collapse of the fibers in the cross-sectional SEM method may also be affected by the later part of the sample preparation; Fast liquid nitrogen dry freezing is supposed to reflect on the fibers' wet stage properties, but it is possible that the sample preparation process, including one hour oven drying, results in differences between wet and dry frozen samples that induced differences between the FiberLab and cross-sectional image analysis methods.

The cross-sectional SEM image analysis method measured properties of fiber wall and width from one direction, similar to the FiberLab cross-section camera. In both methods, the calculation algorithms are based on the approximation that the fiber is circular. Fibers are seldom fully symmetrical in their cross-sectional shape, due to both different degrees of collapse and inherent fiber dimensions and this may have been reflected in the measurement. Measurements of fiber width should be especially affected by the angle at which a partly collapsed fiber is measured. It is likely that this had higher impact on the results when the measurement was based on 600 fibers, as in the cross-sectional SEM image analysis, than when based on 60 000 fibers as the results from the FiberLab device.

Samples of TMP1-3 were also analyzed in a MorFi Lab device for fiber width. The MorFi Lab results were measured on the whole P16/R30 fraction, without the raw data selection process. For comparison, the averages from the FiberLab *in this case* also include all measured material, i.e. also particles without intact fiber walls, e.g. parts of fibrils. Fiber width index as measured in the FiberLab and in the MorFi Lab are shown in *Fig 15*. The MorFi Lab data supported the ranking of the pulps with respect to fiber width obtained from the FiberLab. A linear correlation was seen between fiber width index measured from the FiberLab and fiber width index measured from the MorFi Lab, although data were on different levels.

The results from the FiberLab followed the expected results of the hydrocyclone fractionation (Karnis 1981, Kure et al. 1999, Shagaev and Bergström 2005) and the

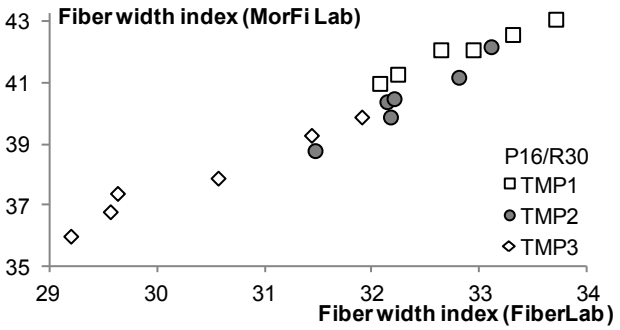

Fig 15. Correlation between fiber width index measured in FiberLab and MorFi Lab optical analyzers for the P16/R30 fractions of the hydrocyclone fractionated pulps.

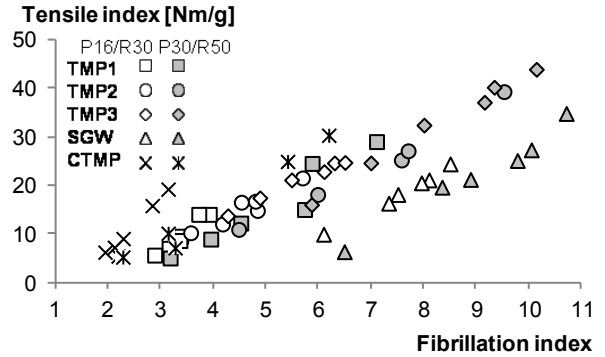

Fig 16a. Long fiber tensile index as a function of fibrillation index of the P16/R30 and P30/R30 fractions of the hydrocyclone fractionated pulps showed that increased fibrillation index correlated with increased tensile index. At a given tensile index, the SGW fibers showed higher fibrillation index than the TMP fibers, and the fibers from the CTMP fractions lower fibrillation index.

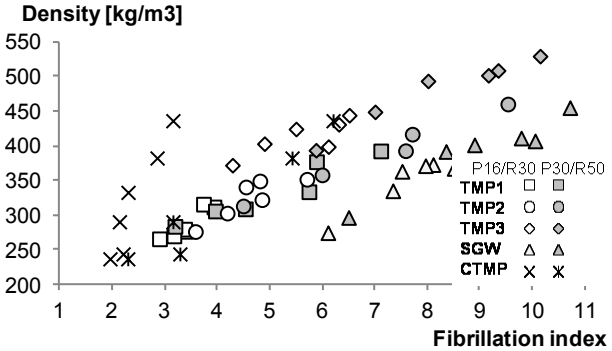

Fig 16b. Long fiber sheet density as a function of fibrillation index of the P16/R30 and P30/R30 fractions of the hydrocyclone fractionated pulps showed that the SGW fibers had a higher fibrillation index at a given density than the TMPs and the CTMP fibers. The evaluated CTMP P16/R30 fractions also seemed to develop density with significantly less influence from fibrillation index than the rest of the evaluated pulps, to rather high levels of sheet density.

MorFi Lab analyzer showed high correlation to the FiberLab results with respect to fiber width index. Both optical analyzers measure relative values and the differences in level were expected. The correlation between fiber width index as measured in FiberLab and fiber width index as measured in the MorFi Lab was higher than the correlation between fiber width from

FiberLab and the cross-sectional SEM image analysis method (c.f. *Fig 14b*).

Based on results of the cross-sectional SEM image analysis method used in this study, FiberLab results were found to show more logical results than the cross-sectional SEM image analysis method, however expressed as relative values.

Correlation between fiber dimensions and sheet properties

In the following figures, the tensile index of handsheets made of long fiber fractions is compared to arithmetic averages of fiber dimensions as evaluated in FiberLab. All FiberLab averages are based on fibers with intact fiber walls to exclude the influence of fines or parts of fibrils. The correlation between tensile index and density (c.f. *Fig 7*) suggests similar influence of fiber dimensions on the long fiber sheet density as on the tensile index. It was deliberately avoided to state the coefficient of determination (R^2) in most correlations in this study. It is not always clear which pulp types should be grouped in different correlations and the focus should be put on the general picture rather than on R^2-values. The influence of fibrillation index on long fiber tensile index for the five pulps is shown in *Fig 16a*.

The slope of correlation between fibrillation index and tensile index of the P16/R30 and P30/R50 fractions appears constant for all pulp fractions except one, but on different levels. The P16/R30 CTMP fibers gave a steeper development of tensile index with increased fibrillation index. At a given tensile index, the CTMP fibers showed a lower fibrillation index than the SGW and TMP fibers. The CTMP P30/R50 fraction followed the slope of the TMP rather than the slope of the coarser CTMP P16/R30 fraction.

Both the P16/R30 and P30/R50 fractions of the SGW pulp showed higher fibrillation index at a given tensile index than the TMP fibers. This was expected since the SGW process typically gives fibers of high specific surface area.

For most fiber properties, the correlation between the fiber properties and sheet properties was very similar for tensile index and density. The correlation between density and fibrillation index, *Fig 16b*, resembled that for tensile index, *Fig 16a,* but the differences between the pulp fractions were somewhat more obvious. The sheet density of the CTMP P16/R30 fraction was higher than the sheet density CTMP P30/R50 fraction and all the other pulps at a given fibrillation index. This was also the case for tensile index (*Fig 16a*). This suggests that the tensile index and density for the CTMP P16/R30 fraction was affected by other fiber properties, e.g. dimensions, than fibrillation index, whereas the P30/R50 fraction seemed to follow the same pattern as the TMPs and the same slope of correlation for both tensile index and density as the TMPs and SGW. The high energy SC grade TMP, TMP3, had a slightly lower fibrillation index at a given density than the two TMPs of lower energy. This was also seen in the tensile index – density correlation (c.f. *Fig 7*) where the high energy TMP showed higher density at a given tensile index.

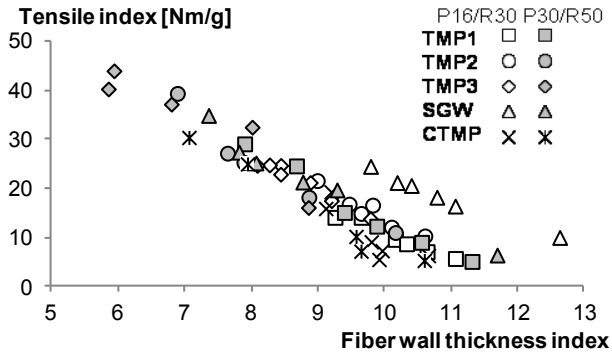

Fig 17. Long fiber tensile index as a function of fibre wall thickness index for the P16/R30 and P30/R30 fractions of the hydrocyclone fractionated pulps. A clear correlation between the tensile index of laboratory sheets and the fiber wall thickness index was found where the tensile index increased with thinner fiber wall thickness for all pulps.

To reach a given long fiber tensile index, it seems that higher fibrillation index was needed for the SGW compared to the TMP, and lower for the CTMP (*Fig 16a*). The SGW fibers' higher collapse resistance index (c.f. *Fig 10a* and *b*) as compared to the other evaluated pulps may be an indication that the SGW fibers are stiffer than the TMPs and CTMP and therefore require external fibrillation to reach a certain tensile index. For CTMP, a lower fibrillation index than for TMP and SGW was observed at a given tensile index or density, and for the CTMP, differences in fibrillation index, especially for the P16/R30 fraction, were small between the five hydrocyclone streams. The low degree of external fibrillation of CTMP fibers was expected, it is well established that compared to the TMP or SGW processes, the CTMP process results in a smoother, more intact fiber surface (Htun and Salmén 1996).

The long fiber tensile index as a function of fiber wall thickness index is shown in *Fig 17*. For all pulps, higher fiber wall thickness index resulted in lower tensile index. For the CTMP P16/R30 fraction, the differences between the hydrocyclone streams were small, as in the case of fibrillation index, c.f. *Fig11a, 11b, 16a*. The SGW P16/R30 fibers showed the same slope in the correlation between fiber wall thickness index and tensile index but on a higher wall thickness level than the other pulps.

In FiberLab, a certain level of grey-scale around the fibers in the images is defined as "fibrillation". Apart from their total projected area, the image analysis does not take the nature of the "fibrillation" into account. It is possible that broken fiber parts from the torn SGW fibers are registered as fibrils which are quite different to the "fibrillation" of the surface of the TMP fibers, and also created in a different way, i.e. without a similar decrease in wall thickness.

Below is the long fiber tensile index plotted against fiber width index, *Fig 18*. The correlation was more scattered than for fiber wall thickness index but it seems like also the relation between width index and tensile index is on another level for the P16/R30 SGW fibers compared to the rest of the pulps. At a given tensile index, the fiber width was the highest for the P16/R30

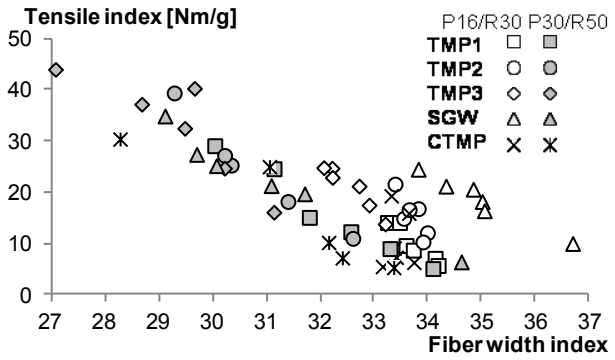

Fig 18. Correlation between long fiber tensile index and arithmetic averages of fiber width index for the P16/R30 and P30/R50 fractions of the evaluated pulps. The correlation between tensile index and fiber width was more scattered than corresponding correlation between tensile index and fiber wall thickness and indicates that at a given tensile index, the P16/R30 fraction fibers measured higher fiber width index than the P30/R50 fraction fibers.

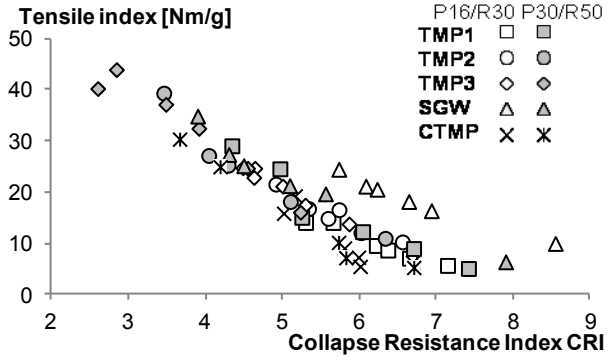

Fig 19. Long fiber tensile index as a function of collapse resistance index, CRI, showed that an increase in collapse resistance index correlated with a lower long fiber tensile index. At a given tensile index, the SGW P16/R30 fraction had a higher collapse resistance index than the SGW P30/R50 fraction and all fractions of the TMPs, whereas the CTMP fibers collapse resistance index was lower.

SGW fibers. This is similar to the results in the previous figure (*Fig 17*). In *Fig 18* also shows that at a given tensile index, the P16/R30 fibers had higher fiber width than the P30/R50 fibers for all pulps. This is further discussed below (*Fig 20,21*).

Long fiber tensile index as a function of collapse resistance index is found in *Fig 19*. The collapse resistance index was calculated from FiberLab fiber width index and fiber wall thickness index (*Eq 1*). The collapse resistance index showed a higher and more linear correlation to tensile index (*Fig 19*) than fiber width, probably a result of the influence of fiber wall thickness on the collapse resistance index. The correlation to tensile index was also very similar to that of fiber wall thickness index (c.f. *Fig 17*).

When the collapse resistance index increased, long fiber tensile index decreased in the same way for all tested pulps, *Fig 19*. The P16/R30 SGW fibers showed a higher collapse resistance index at a given tensile index as was expected based on the results of the fiber wall thickness and fiber width (c.f. *Fig 17, 18*). Differences in measured sheet properties also appeared larger at higher collapse resistance index levels than at lower.

It seems that for the SGW fibers, particularly the P16/R30 fraction, fibrillation index (c.f. *Fig 16*) was the fiber dimension which contributed the most to long fiber tensile index (and density) amongst the fiber dimensions evaluated in this study. At a given tensile index, the CTMP showed the lowest collapse resistance index. Further, for CTMP, tensile index and density seemed to be less dependent on fibrillation index and more on fiber wall thickness and collapse resistance index than the TMPs and the SGW. It is possible that this is due to the more flexible nature of the chemically pretreated CTMP fibers as compared to the stiffer SGW fibers, with the TMP fibers somewhere between them. The CTMP P16/R30 fraction showed rather small differences in fibrillation index, fiber wall thickness, fiber width and collapse resistance index (c.f. *Fig 16-19*) between the hydrocyclone streams. The results however indicate a different slope for the P16/R30 CTMP fraction in the

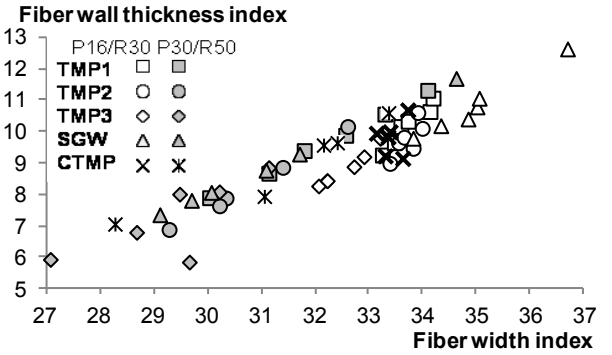

Fig 20. Correlation between fiber width index and fiber wall thickness index analyzed in FiberLab. Differences in fiber width for the P16/R30 CTMP fibers were very small which was also seen in the SEM image analysis. The correlation between fiber wall thickness index and fiber width index was linear but seems to be on two different levels for the P30/R50 and P16/R30 fractions, which at a given fiber width had lower fiber wall thickness than fibers from the P30/R50 fraction.

correlation between the evaluated fiber dimensions and long fiber sheet tensile index and density, an observation which would benefit from further studies.

To get more information about the refining and grinding's influence on the fiber dimensions in the different processes, fiber dimensions were compared to each other. The correlation between the P16/R30 and P30/R50 fiber width index and fiber wall thickness index for all pulps are seen in *Fig 20*. For the CTMP P16/R30 fraction (marked in bold in *Fig 20*), very small differences were measured in fiber width. It should also be noted that there is a very high correlation between collapse resistance index and wall thickness index, whereas the correlation between collapse resistance index and fiber width is weaker.

Fig 20 shows an indication of two different levels for the P16/R30 and P30/R50 fractions in the linear correlation between fiber width and fiber wall thickness as evaluated in the FiberLab device. This was also seen for the correlation between fiber width index and tensile index (*Fig 18)* but not in the correlation between collapse resistance index and tensile index (*Fig 19*) where both

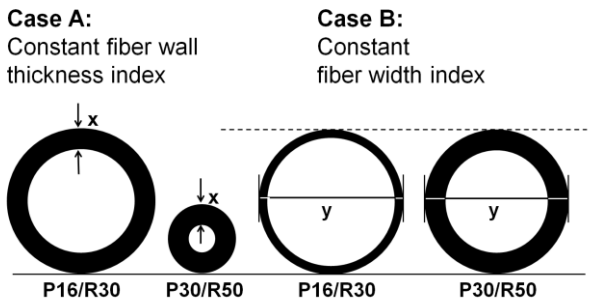

Fig 21. Outline of different fiber types with constant fiber wall thickness index but different fiber width index (case A) and constant fiber width index but different fiber wall thickness index (case B).

fractions show the same linear behaviour. It is possible that the high influence of fiber wall thickness on the collapse resistance index (*Eq 1*) reduces differences introduced by fiber width.

Fig 18 and *Fig 20* suggest that for a given fiber wall thickness, the P16/R30 fraction fibers had higher fiber width than the P30/R50 fraction fibers (case A, *Fig 21*), or at a given fiber width, the P16/R30 fraction fibers had thinner fiber wall thickness than the P30/R50 fraction fibers (case B, *Fig 21*). According to the results of the averages seen in *Fig 20*, this would then result in more easily collapsed fibers from the P16/R30 fractions than from the P30/R50 fractions. The P30/R50 fraction generally produces sheets of higher tensile index and density than the P16/R30 fraction (c.f. *Fig 7*). It is possible that this is an effect of that the shorter P30/R50 fraction fibers are easier to pack in a sheet than the longer P16/R30 fraction fibers, thus contributing to higher density and tensile index. The middle fraction material without intact fiber walls found in the P30/R50 fraction may also be the reason behind higher tensile index and density in the P30/R50 fraction compared to the P16/R30 fraction, rather than flexibility and collapsibility of intact fibers.

It can be speculated whether extensive refiner or grinder treatment have resulted in fiber shortening of some fibers which then may have ended up in the shorter P30/R50 fraction without the same degree of wall treatment. This could be due to some inherent fiber quality which makes the fibers more durable, so they can endure fiber wall treatment without breakage, these fibers would then be found in the P16/R30 fraction. Or it could be a coincidence from the measured averages. Further, if the earlywood fibers of larger diameters and thinner fiber walls are more flexible and resistant to fiber breakage, it is possible that this fiber type is over represented in the P16/R30 fraction; this would benefit from further studies.

Fig 22 shows the correlations between fibrillation index and fiber wall thickness index. For a given fiber wall thickness index, the fibrillation index of the SGW fibers was significantly higher than for the TMP fibers, and also showed a less steep slope. Differences in fiber wall thickness index between SGW and TMP fibers appeared larger at low fibrillation index levels, than at high. For the CTMP fibers, the fibrillation index at a given wall

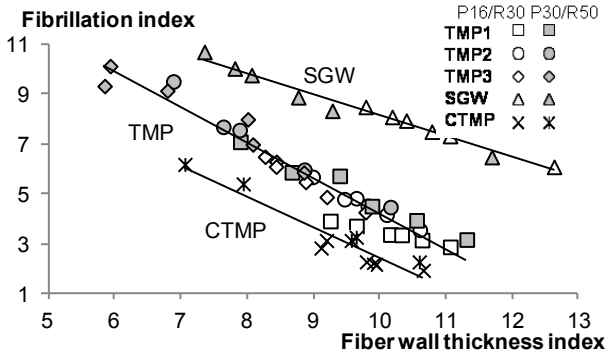

Fig 22. Relation between fibrillation index and fiber wall thickness index showed different levels for the three pulp types, where at a given fiber wall thickness index, the SGW fibers had the highest fibrillation index, the CTMP fibers the lowest and the TMP fibers were placed between the SGW and CTMP.

thickness index was lower overall than for the TMP fibers. It is likely that the fiber wall softening in the CTMP process results in a lower fibrillation index compared with the SGW and TMP processes. The FiberLab evaluations reflect on the area of external fibrils, not on the type of fibrils. It is possible that the SGW fibers have flake-like fibrils already created in the defibration process, which will result in a high fibrillation index from the FiberLab evaluations. The shape and quality of the fine material of the various pulps is outside the scope of this study and will not be further discussed. It is also possible that broken fiber parts, still attached to the fiber, are evaluated as area of external fibrils in the FiberLab device.

BIN – a combination of fiber dimensions

None of the evaluated parameters: fiber wall thickness index, fiber width index, collapse resistance index or fibrillation index, fully correlated to long fiber tensile index or density for the fractions of the five pulps. Linear regressions were therefore made where averages of fibrillation index and collapse resistance index, CRI, was related to long fiber tensile index for the P16/R30 fractions of TMP1 and TMP2, streams 0-5 (feed plus the five hydrocyclone stages). This linear regression resulted in constants which together with collapse resistance index CRI (based on fiber wall thickness index and fiber width index) and fibrillation index formed the equation for BIN, short for "*B*onding ability *IN*fluence", *Eq 3*.

$$BIN = A + B * Collapse\,resist.idx + C * Fibrill.idx \qquad [3]$$

Levels of fiber wall thickness index, fiber width index, collapse resistance index and fibrillation index are not absolute for all optical measurement devices but differ depending on the specific optical measurement device, software, calibration settings and sample preparation standards. Since relations between the coefficients in *Eq 3*, *A*, *B*, and *C* may also differ because of these differences, intervals for the coefficients are given below. These were obtained for evaluations with different software calibrations in the FiberLab device currently used. For FiberLab settings and calibrations used in this study, *A* was between 15 and 30, *B* between -4 and -2 and *C* between 1 and 4.

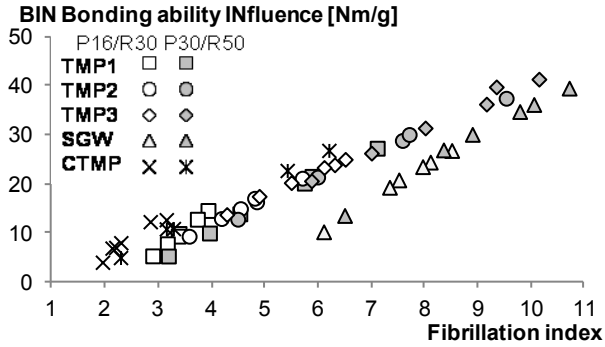

Fig 23a. *BIN*, Bonding Ability Influence, as a function of fibrillation index showed higher fibrillation index for a given BIN for the SGW pulp than for the TMP, and slightly lower fibrillation for the CTMP fibers.

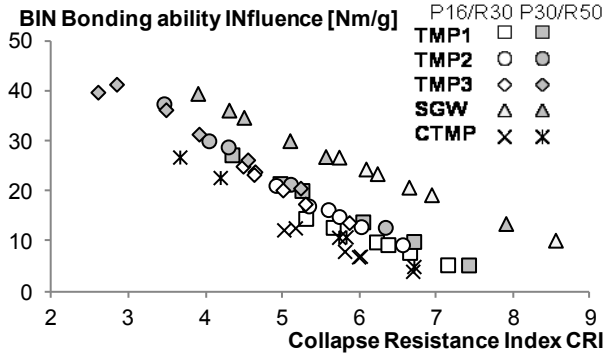

Fig 23b. *BIN*, Bonding Ability Influence, as a function of collapse resistance index CRI showed that at a given BIN the three pulps showed three different levels of collapse resistance index where the SGW fibers had the highest CRI, followed by the TMP fibers and the CTMP fibers which had the lowest collapse resistance index at a given BIN value.

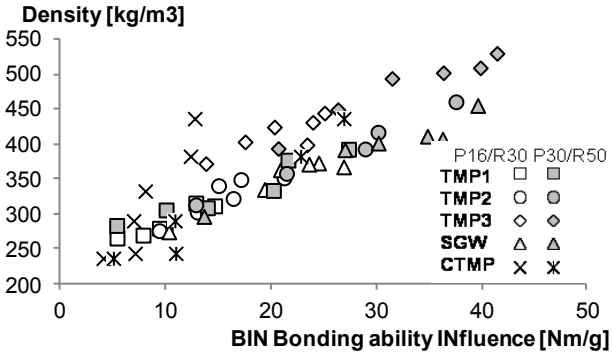

Fig 24a. The relation between BIN and long fiber density of the P16/R30 and P30/R50 fractions showed a more linear but slightly scattered correlation for all pulps, with the exception of the CTMP P16/R30 fraction.

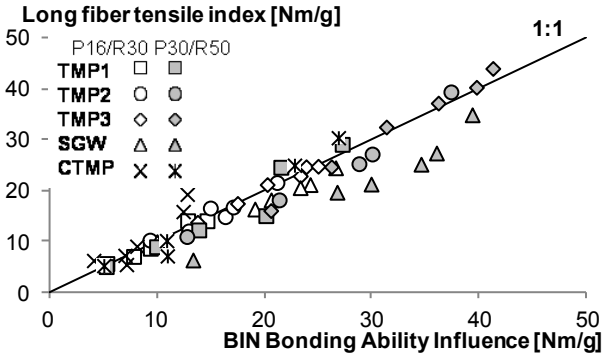

Fig 24b. Using the *BIN* (Bonding Ability Influence) equation on the P16/R30 and P30/R50 fractions on all evaluated pulps gave a linear correlation between BIN and the long fiber tensile index. For all pulps with the exception of the SGW P30/R50 fraction, the long fiber tensile index could be derived by the same equation of collapse resistance index CRI and fibrillation index from optical measurements of individual fibers.

The diversity of mechanical pulp fibers is large, both as a result of inherent raw material dimensions and process conditions (Ferritsius et al. 2009). Following the increasing demand on final product quality, each fiber's property is becoming more and more important for product quality as well as process optimization. Averages of the whole pulps may not be sufficient, by characterizing each individual fiber, a more complete view is gained of the fibers in a pulp. The value of Bonding Ability Influence, *BIN*, was calculated from the FiberLab raw data for each fiber where the cross-sectional wall area, fibrillation index or curl was possible to determine, i.e. not reported as zero in the data file. As *BIN* was originally calculated from averages, also negative *BIN* values were derived for some fibers. All *BIN* values are to be recognized as indexes as for the FiberLab fiber dimensions. Correlations between *BIN* and fibrillation index (*Fig 23a*) and *BIN* and Collapse resistance Index *CRI* (*Fig 23b*) are found below. For both fibrillation index and collapse resistance index, the correlations to *BIN* were on different levels for the SGW, TMP and CTMP pulp types. To achieve a given *BIN* value, the three different TMPs (CD refined news grade, DD refined news grade and DD refined SC grade) were well aligned, with the same increase of *BIN* for increased fibrillation index and the same decrease in *BIN* for increased collapse resistance index. The CTMP fibers needed lower fibrillation index and lower collapse resistance index to achieve a certain *BIN* whereas the SGW fibers could reach this level of *BIN* at a higher collapse resistance index but also at a higher fibrillation index.

The *BIN* equation was originally derived to correlate to long fiber tensile index, *Eq 3*, from linear regressions using fiber dimensions and tensile index of the P16/R30 fractions of twelve pulps (feed and five hydrocyclone fractionated streams) of TMP1 and TMP2. When results also from the P30/R50 fractions of TMP1 and TMP2 (fiber data and long fiber tensile index) were used for the existing *BIN* equation, *Eq 3*, a similar correlation between BIN and long fiber tensile index for the P30/R50 fractions as for the P16/R30 fractions were seen, *Fig 24b*. This indicates the same influence of fiber dimensions on long fiber tensile index for the P30/R50 fraction as for the P16/R30 fraction. With the exception of SGW P30/R50 fraction, the same relationship was also seen for the rest of the pulps, both P16/R30 and P30/R50 fractions, *Fig 24b*. The correlation between long fiber tensile index and density was earlier seen to be rather high for the evaluated fractions (c.f. *Fig 7*). The correlation between *BIN* and long fiber density is shown in *Fig 24a*. The correlation was linear for all pulps except the P16/R30

CTMP fraction however on different levels. At a given BIN, the SC grade TMP, TMP3, showed higher density, which was also seen in the correlation between tensile index and density (*Fig 7*).

For *BIN* correlated to the long fiber density, separate levels for the TMP3 and the CTMP fibers were observed (*Fig 24a*) whereas for *BIN* correlated to tensile index (*Fig 24b*), the correlation was more linear around the same line for all the evaluated pulps. For the SGW fibers, it seemed that the longer fibers, from the SGW P16/R30 fraction, showed the same correlation between *BIN* and tensile index as the TMP fibers, whereas the shorter SGW P30/R50 fibers were predicted to influence the long fiber sheet tensile index slightly more than measured.

The consequent (except the SGW P30/R50 fraction) correlation between BIN, calculated from optical measurements of fiber wall thickness, fiber width, and external fibrillation of individual fibers, and long fiber tensile index of handsheets of the various pulp types and various fiber fractions, showed that the fiber dimensions which separately correlate with tensile index on slightly different levels can correlate in the same way when combined.

Discussion

This study was aiming at investigating which fiber properties that influence long fiber tensile index and density in mechanical pulps. Improved knowledge of this should increase the understanding of and the possibility to optimize the effect of mechanical pulping processes on the final pulp quality.

The study was based on five pulps, separated in hydrocyclones and in a Bauer McNett fractionator to achieve a broader range of pulp properties. Long fiber sheets were made from each hydrocyclone stream and Bauer McNett fraction and fiber dimensions from these fractions were independently compared to the tensile index and density of the produced sheets. All testing was performed in a research laboratory with high standards and well established testing accuracy and repeatability.

From the laboratory sheet testing of the fractionated pulps, it was found that differences in long fiber tensile index and density between first hydrocyclone accept (stream 1) and last hydrocyclone reject (stream 5) were higher for the P30/R50 fraction, than for the P16/R30 fraction. This may reflect either that the hydrocyclones fractionate shorter fibers more efficiently than longer fibers, or that the P30/R50 fraction contains fibers of more varying degrees of fiber development. The width of the distribution of fiber wall thickness and fibrillation index evaluated as F0.90, the difference between percentile 0.05 and percentile 0.95 (*Eq 2*) showed that for the evaluated pulps, the P30/R50 fraction had a wider distribution in fibrillation index than the P16/R30 fraction, but a more narrow distribution in fiber wall thickness index. As fibrillation index was found to have a major influence on evaluated sheet properties, especially tensile index, the wider distribution in fibrillation index may be the reason for the larger differences between the hydrocyclone streams for the P30/R50 fraction.

Cross-sectional SEM image analysis and FiberLab analysis ranked hydrocyclone fractionated samples equally for fiber wall thickness index but showed some different rankings in evaluations of fiber width. The two methods also showed some differences in ranking between the pulps. Differences in fiber width between the hydrocyclone streams for two of the analyzed samples were very small which may have been the reason for the different rankings between FiberLab and the cross-sectional SEM method. The different ranking for two pulps was not considered to affect the final conclusions of this work. Evaluations of fiber width index using the MorFi Lab analyzer showed high correlation with the FiberLab results, which were also in agreement with literature about how fibers divide in hydrocyclones with respect to fiber wall thickness (Karnis 1981, Kure et al. 1999, Shagaev and Bergström 2005). The semi-automatic cross-sectional SEM image analysis method used in this study was considered less trustworthy than the optical measurements, also due to the low number of measured fibers, 600 in the cross-sectional SEM image analysis method compared to 60 000 in the FiberLab method. To fully investigate the nature of the differences between the cross sectional SEM analysis method and the FiberLab method, more samples should be analyzed with a larger number of measured fibers. It should be noted that despite making comparisons with the cross-sectional SEM image analysis method used by Reme (2000) and Reme and Helle (2001), there are some differences between that method and the one used here.

Differences reflected in long fiber laboratory sheet properties between the hydrocyclone streams were mainly reflected in fibrillation index and fiber wall thickness. Fiber width showed some correlation to sheet properties when used as a single parameter but greater when combined with fiber wall thickness into collapse resistance index. This should be taken into consideration in future development of optical analyzers, as most market analyzers today offer measurement only of fiber width and not fiber wall thickness. Indications were seen that at a given fiber width index fibers from the P16/R30 fraction had thinner fiber walls than the P30/R50 fraction fibers, suggesting that the P16/R30 fraction fibers would be easier to collapse. This observation needs further evaluation.

Throughout all results reflecting on fiber dimensions, a broad range of fiber properties within each sample was observed, on feed pulps as well as in hydrocyclone streams. The correlation between fiber properties e.g. fiber wall thickness index and fibrillation index and sheet properties was often found to change with the same slope for the evaluated pulps, despite starting at different levels. This further induces the need to consider distributions of fiber properties in fiber evaluations, at least as a complement to average values. To make the most of samples evaluated in optical analyzers, both when evaluating averages and distributions of fiber dimensions, raw data is to be preferred over standard average values calculated in the instrument. This offers greater possibilities of retrieving more information from post-measurement calculations of fiber dimensions e.g. collapse resistance index CRI and distributions of various

fiber dimensions. It also enables to control the content of the average value and to divide the data prior evaluation, e.g. to look into the development of particularly thick-walled fibers over a given process stage, or to evaluate the behaviour of the most fibrillated fibers before or after a process change. Further, considering the wide distribution of fiber dimensions in mechanical pulps, the number of fibers on which results are based should always be considered so that it is sufficiently high for a valid fiber characterization and to support any conclusions.

Neither of the measured and calculated fiber dimensions fibrillation index, fiber wall thickness index, fiber width index or collapse resistance index showed a linear correlation to long fiber sheet tensile index or density for all pulps. When the collapse resistance index CRI (calculated for each fiber from fiber wall thickness and fiber width) and fibrillation index was combined into the factor *BIN*, Bonding ability INfluence, all pulps except the SGW P30/R50 fraction followed the same linear correlation to long fiber tensile index. BIN was calculated from linear regressions of the P16/R30 fractions of hydrocyclone fractionated TMP1 and TMP2 (feed plus five streams for each pulp), and showed the same linear correlation to tensile index when used for the other pulps used in this study, both for the P16/R30 and the P30/R50 fractions. To be able to evaluate each fiber's bonding ability, the BIN equation can be applied on individual fibers from which distributions can be made.

The results from this study and the method of combining fiber dimensions into one common factor may be beneficial in future development of methods for process control. Work is also ongoing in which the fiber dimensions are combined into one common factor by other means than linear regressions (Ferritsius et al. 2009). Final products are made from fibers, and it is the fiber properties that will affect the final product properties. The intermediary stage of producing long fiber laboratory sheets for fiber characterization is time consuming and difficult to fit into mill testing. There is also a risk of introducing laboratory and technician dependent results which may have large consequences if used for evaluation and steering of the process. Further, the possible relations between handsheet properties and final product properties are not always straight-forward (Klinga 2007). The potential of rapid optical analyzers independent of handling methods should be used to a higher degree. The development of optical analyzers to involve external fibrillation, fiber wall thickness and possibly also internal fibrillation as a complement to fiber width and fiber length is highly encouraged.

Conclusions

This study regarding the influence of fiber dimensions on long fiber laboratory sheet properties of three different TMPs, one SGW and one CTMP showed that:

- The influence of fiber dimensions on sheet properties evaluated in this study was different for fibers from different process types.
- Fiber dimensions from FiberLab optical analyzer followed expected rankings with respect to mechanical pulp process type and hydrocyclone fractionation. FiberLab results correlated with results from MorFi Lab optical analyzer regarding fiber width.
- There was no clear correlation between the FiberLab and the cross-sectional SEM image analysis methods for fiber width, where the differences between the samples were small. For fiber wall thickness, the correlation was higher but on different levels for different pulps.
- FiberLab evaluations showed that fibrillation index had a positive influence on tensile index and density of sheets from long fiber fractions whereas fiber wall thickness index, fiber width and collapse resistance index had a negative influence. This was observed for the five evaluated pulps, although at different levels.
- To develop tensile index and density of sheets from long fiber fractions, the degree of fibrillation index of the fibers seemed have the highest influence for the SGW fibers, whereas a low collapse resistance index seemed the most important for the CTMP fibers. The three TMPs were found between the SGW and the CTMP.
- Collapse resistance index CRI, calculated from fiber wall thickness index and fiber width index, and fibrillation index were combined into a novel factor - *BIN*, short for *B*onding ability *IN*fluence. *BIN* correlated well to tensile index of sheets from long fibers and resulted in a linear correlation with long fiber sheet tensile index. With the exception of the SGW P30/R50 fraction, the P16/R30 and the P30/R50 fractions of all five pulps followed the same linear equation for *BIN*.
- The combination of fiber dimensions into one common factor provided more accurate predictions of sheet properties than did the fiber dimensions separately.
- The *BIN* method should be a useful tool for detailed evaluation and characterization of fibers of various mechanical pulps.

Acknowledgements

Noss AB is acknowledged for enabling and skilfully carrying out the pilot plant hydrocyclone fractionation, Alf Gustafsson, Olle Henningson, Örjan Sävborg, Stora Enso, are specifically acknowledged for careful laboratory work and Hans Ersson, Stora Enso Kvarnsveden for valuable discussion and support. Michel Petit-Conil, CTP, and Michael Lecourt, FCBA, Grenoble, France, are acknowledged for enabling fiber testing in the MorFi Lab. Operators, laboratory technicians and development engineers at all involved Stora Enso mills are acknowledged for assisting in sampling and testing. Hans Höglund, Mats Rundlöf and Per Engstrand are acknowledged for valuable comments on the manuscript. The Swedish Knowledge Foundation is acknowledged for financial support through the Mid Sweden University FSCN Mechanical Pulp Research College.

Literature

Eymin Petot Tourtollet G., Cottin, F., Cochaux, A., Petit-Conil, M. (2003): "The use of Morfi analyser to characterise mechanical pulps", Proceedings, Int. Mechanical Pulping Conf., Quebec, Canada

Ferritsius, O. (1996): "Control of fundamental pulp parameters in TMP and SGW production by the use of factor analysis", Proceedings, Swedish Association of Pulp and Paper Engineers conference, Stockholm, Sweden

Ferritsius, O., Ferritsius, R. (1997): "Improved quality control and process design in production of mechanical pulp by the use of factor analysis", Proceedings, Int. Mechanical Pulping Conf., Stockholm, Sweden, 111-125

Ferritsius, O., Ferritsius, R. (2001): "Experiences from Stora Enso mills of Using Factor Analysis for Control of pulp and Paper Quality", Proceedings, Int. Mechanical Pulping Conf., Helsinki, Finland, 495-504

Ferritsius, O., Ferritsius, R., Reyier, S. (2009): "The influence of process design on the distribution of fundamental fibre parameters", Proceedings, Int. mech. Pulp. Conf., Sundsvall, Sweden, 292-297

Forgacs, O.L. (1963): "The Characterization of Mechanical Pulps", Pulp and Paper Magazine of Canada, 64, T89-T116

Htun, M., Salmén, L. (1996): "The importance of understanding the physical and chemical properties of wood to acheive energy efficiency in mechanical pulping", Wochenblatt für Papierfabrikation, 124(6): 232

Höglund, H., Wilhemsson, K. (1993): The product must determine the choice of wood type in mechanical pulping", Proceedings, Int. Mechanical Pulping Conf., Oslo, Norway

Kajaani FiberLab™ Operating Manual (2002), W4230467V3.5 EN, Metso Automation

Karnis, A. (1981): "Refining of mechanical pulp rejects", Proceedings, Int. Mechanical Pulping Conf., Oslo, Norway

Kauppinen, M. (1998): "Prediction and Control of Paper Properties by Fiber Width and Cell Wall Thickness Measurement with Fast Image Analysis", PTS Symposium: Image analysis for Quality and Enhanced productivity.

Klinga, N. (2007): "The influence of fibre characteristics on bulk and strength properties of TMP and CTMP from spruce", Licentiate thesis, Mid Sweden University, Sweden

Kure, K.-A., Dahlqvist, G., Helle, T. (1999): "Morphological characteristics of TMP fibres as affected by the rotational speed of the refiner", Nordic Pulp and Paper Research Journal, 14(2), 105-109

Lhotta, T., Villforth, K., Schabel, S. (2007): "Fibre Classification - Advanced Fibre Analysis for Quality Control and process Optimization in Stock preparation", Das Papier, (3)T25-28

Mohlin, U.-B. (1980): "Properties of TMP fractions and their importance for the quality of printing papers", Svensk Papperstidning #16, 461-466

Mohlin, U.-B. (1989): "Fibre bonding ability - a key pulp parameter for mechanical pulps to be used in printing papers", Int. Mechanical Pulping Conf., Helsinki, Finland

Mohlin, U.-B. (1997): "Fibre development during mechanical pulp refining", J Pulp pap. Sci., 23(1): J28-J33

Petit-Conil, M., Cochaux, A., de Choudens, C. (1994): "Mechanical pulp characterization: a new and rapid method to evaluate fiber flexibility", Paper and Timber (Pap Puu), 76(10), 657-662

Reme, P.A. (2000): "Some effects of wood characteristics and the pulping process on mechanical pulp fibres", PhD Thesis, Norwegian University of Science and Technology, Trondheim, Norway

Reme, P.A., Helle, T. (2001): "Quantitative Assessment of Mechanical Fibre Dimensions During Defibration and Fibre Development", Journal of Pulp and Paper Science, 27(1), 1-7

Reyier, S. (2008): "Bonding ability distribution of fibers in mechanical pulp furnishes", Licentiate Thesis, Mid Sweden University, Sundsvall, Sweden

Reyier, S., Ferritsius, O., Shagaev, O. (2008): "Measuring the bonding ability distribution of fibers in mechanical pulps", TAPPI Journal, 7(12), 26-32

Reyier, S., Ferritsius, O., Ferritsius, R. (2011): "The development of fiber characteristic distributions in mechanical pulp refining", Proceedings, Int. Mechanical Pulping Conf., Xi'an, China

Rundlöf, M: (2002): "Interaction of dissolved and colloidal substances with fines of mechanical pulp: influence on sheet properties and basic aspects of adhesion", PhD thesis, Royal Institute of Technology, Sweden

Shagaev, O., and Bergström, B. (2005): "Advanced Process for Production of High Quality Mechanical Pulps for Value-Added Paper Grades." Proceedings, 24th Int. Mechanical Pulping Conf., Oslo, Norway, 169-179

Strand, B. (1987): "Factor Analysis as Applied to the Characterization of High Yield Pulps", TAPPI Pulping Conf. Washington D.C., USA, November 1-5, 1987, 61-66.

Vesterlind, E-L., Höglund, H. (2005): "Chemi-mechanical pulp made from birch at high temperature", Proceedings, SPCI Int. Conference, Stockholm, Sweden.

Manuscript received October 11, 2011

Accepted October 18, 2012